

Supplementary Information for: Photodetachment and Photoreactions of Substituted Naphthalene Anions in a Tandem Ion Mobility Spectrometer

J. N. Bull, J. T. Buntine, M. S. Scholz, E. Carrascosa, L. Giacomozzi,
M. H. Stockett, E. J. Bieske

1 Chemical synthesis

Samples of 2-naphthol and 6-hydroxy-2-naphthoic acid were purchased from Sigma-Aldrich (Castle Hill, >99% purity). The methyl ester, 6-hydroxy-2-methylnaphthoate, was synthesised by Fischer esterification of the acid according to the following procedure. 6-hydroxy-2-naphthoic acid (100 mg, 0.531 mmol) was dissolved in methanol (2 mL) with a trace of H_2SO_4 (cat.). The solution was stirred for ~24 hrs at ~50°C and then neutralised using aqueous NH_3 solution. The final product used for experimental purposes without further purification.

2 Electronic structure calculations

Correctly describing the excited states of naphthalene and related acenes is a challenge for many electronic structure methods. Briefly, linear acenes have D_{2h} point symmetry with a totally symmetric ground electronic state (A_{1g}). There are two low-lying singlet excited states that contribute to the absorption spectrum, L_a with B_{2u} symmetry and L_b with B_{3u} symmetry.¹ The transition dipole moment for excitation from the ground state is directed along the short (L_a) and long (L_b) molecular axes, respectively.² For naphthalene, L_b ($f \approx 0.00$) is lower in energy and has mixed HOMO-1 \rightarrow LUMO and HOMO \rightarrow LUMO+1 character, whereas L_a ($f \approx 0.09$) has HOMO \rightarrow LUMO character.^{3,4} For all larger linear acenes, the ordering of these states is reversed.^{1,5} A series of high-level electronic structure studies has shown the importance of double (and higher order) excitations for describing these states (particularly L_b),^{1,4,5} and demonstrated that most DFT functionals within the TD-DFT framework are inadequate.⁶⁻⁸ Specifically, for naphthalene, the experimental vertical $L_a - L_b$ difference is 0.53 eV, whereas TD-DFT methods such as PBE0, M06-2X, ω B97X-D (aug-cc-pVTZ basis set) give values ranging from -0.1 – 0.1 eV, where a negative indicates an incorrect ordering of the states. In the present paper, we calculated the vertical excitation energies for NPO^- at the EOM-CC3/aug-cc-pVDZ level of theory^{9,10} (MP2/aug-cc-pVDZ optimised geometry) because this level of theory has proven reliable for describing naphthalene and related systems.^{11,12} Calculated values are 2.71 eV for L_a and 2.93 eV for L_b . The EOM-CC2 L_a values for NPOO^- and NPOC^- are 2.98 and 3.97 eV, respectively. Furthermore, because these anions have dipole-bound states and associated low-lying diffuse orbitals, excitation of the L_a and L_b states do not involve transitions to the LUMO or LUMO+1 orbitals, rather the two lowest energy $\pi\pi^*$ orbitals denoted as $1\pi\pi^*$ and $2\pi\pi^*$. Molecular orbitals associated with the $L_a \leftarrow S_0$ and $L_b \leftarrow S_0$ transitions for naphthalene, NPO^- and NPOO^- are shown in Fig. S1.

Excitation profiles for the L_a state of NPO^- and L_a and L_b states of NPOO^- were simulated using time-dependent CAM-B3LYP/aug-cc-pVDZ in the Franck-Condon-Herzberg-Teller (FCHT) framework at 300 K (i.e. including hot bands) as implemented in Gaussian 16.^{13,14} The FCHT model was applied because L_a and L_b states of the naphthalene core are prototypical examples of vibronic activity due to coupled electronic and nuclear motion.^{15,16} The CAM-B3LYP method was chosen because of correct ordering of the L_a and L_b states.

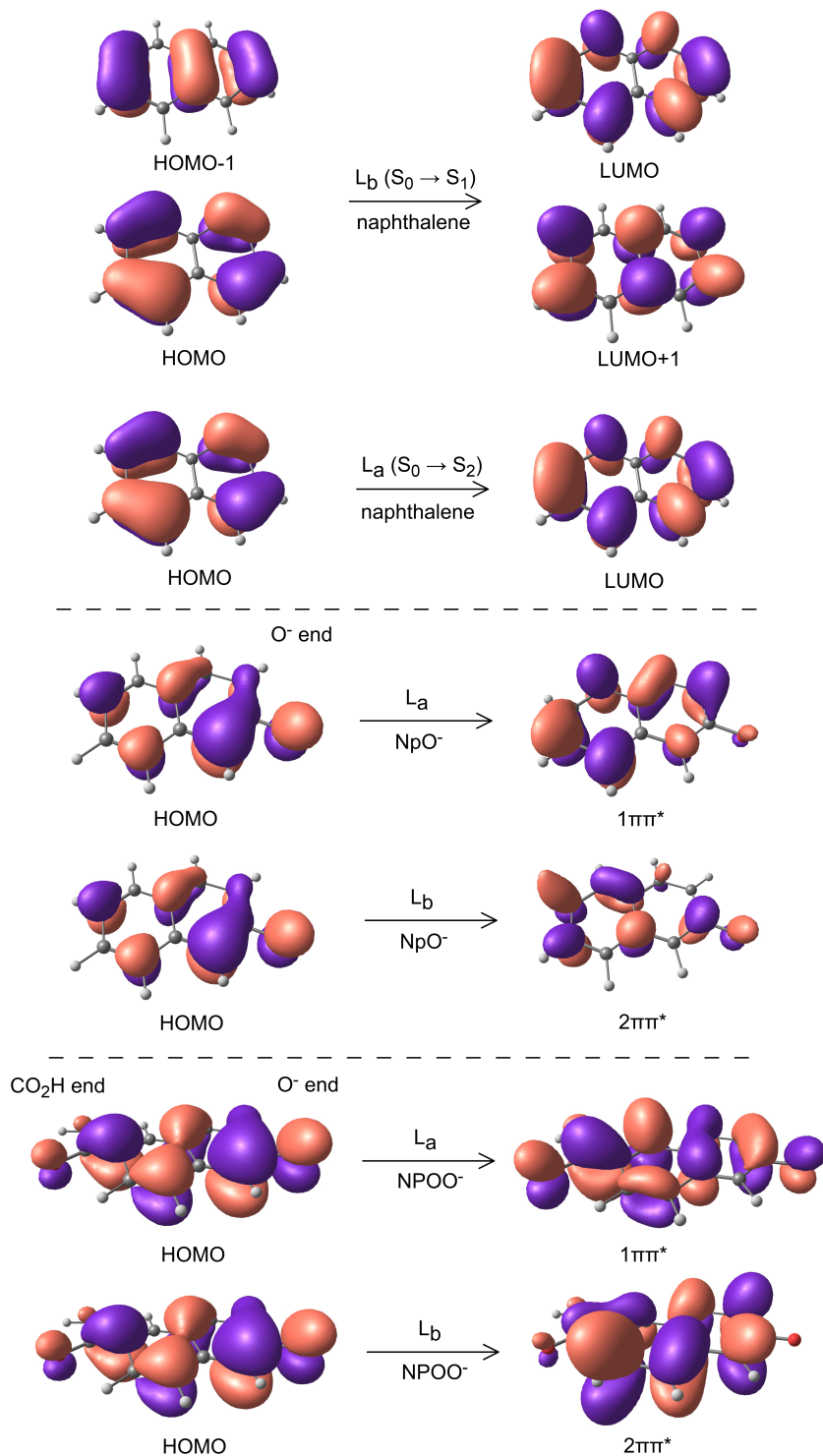


Figure S1: Molecular orbitals associated with the L_a and L_b states of naphthalene (upper), NpO^- (middle), and $NPOO^-$ (lower). For NpO^- and $NPOO^-$, both states predominately involve a one orbital transition.

For NpO^- [Fig. S2(a)], the simulations predicted the $L_a \leftarrow S_0$ band system ($f \approx 0.14$) features a progression dominated by the $\nu_{32}(a') = 437 \text{ cm}^{-1}$ in-plane vibrational mode (Fig. S3a). We did not model the $L_b \leftarrow S_0$ transition ($f \approx 0.02$) for NpO^- because, like naphthalene, this transition has strong double excitation character and requires more a rigorous theoretical treatment. For $NPOO^-$ [Fig. S2(b)], the FCHT simulations predict the $L_a \leftarrow S_0$ transition ($f = 0.31$) has a progression dominated by the $\nu_1(a') = 154 \text{ cm}^{-1}$ in-plane CO_2 wag mode (Fig. S4a). FCHT

simulation of the $L_b \leftarrow S_0$ ($f = 0.28$) transition suggest it is origin dominated, but that at 300 K there are significant hot-band contributions.

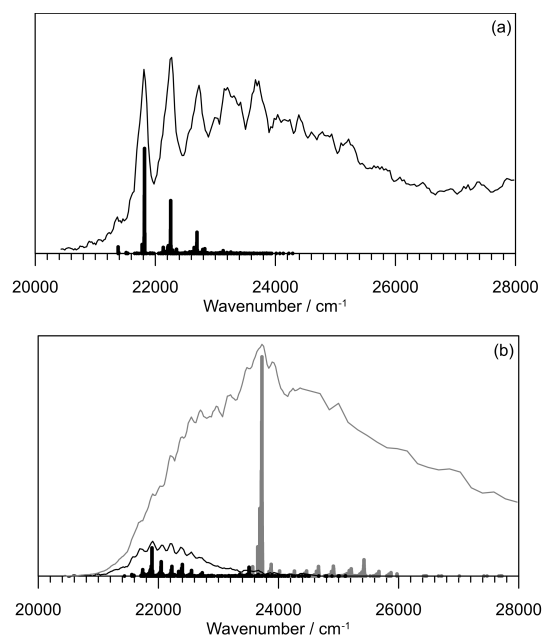


Figure S2: Franck-Condon-Herzberg-Teller simulations: (a) $\text{NPO}^- L_a$, and (b) $\text{NPOO}^- L_a$ (black) and L_b (grey). In both cases, the calculated origins of the L_a and L_b bands have been shifted for best agreement with the experimental spectrum. For NPO^- , the most intense transition agrees well with the EOM-CC3 calculated value for the vertical excitation energy (2.71 eV); the vertical excitation energy for the L_b state is calculated to lie $\sim 1770 \text{ cm}^{-1}$ higher in energy, suggesting the maximum lies at around 23600 cm^{-1} .

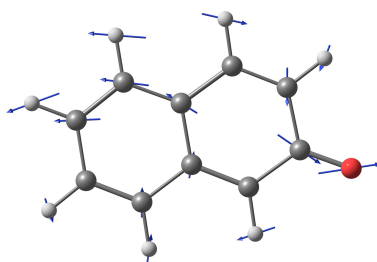


Figure S3: Principal Franck-Condon active mode ($\nu_{32}(a') = 437 \text{ cm}^{-1}$) for the L_a state of NPO^- .

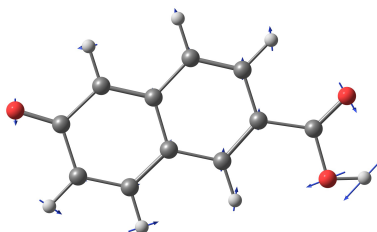


Figure S4: Principal Franck-Condon active mode ($\nu_{39}(a') = 154 \text{ cm}^{-1}$) for the L_a state of NPOO^- .

Mode	Symmetry	S ₀	L _a
1	a'	3196	3227
2	a'	3182	3221
3	a'	3180	3196
4	a'	3169	3195
5	a'	3160	3188
6	a'	3154	3186
7	a'	3141	3179
8	a'	1674	1683
9	a'	1666	1663
10	a'	1616	1609
11	a'	1561	1598
12	a'	1532	1534
13	a'	1494	1493
14	a'	1438	1439
15	a'	1407	1428
16	a'	1404	1384
17	a'	1310	1324
18	a'	1279	1295
19	a'	1242	1247
20	a'	1197	1203
21	a'	1159	1171
22	a'	1147	1155
23	a'	1129	1139
24	a'	1046	1059
25	a'	946	938
26	a'	922	915
27	a'	777	775
28	a'	739	733
29	a'	634	630
30	a'	536	533
31	a'	487	480
32	a'	439	437
33	a'	307	311
34	a''	992	1026
35	a''	999	1048
36	a''	960	1004
37	a''	912	946
38	a''	869	910
39	a''	816	841
40	a''	794	796
41	a''	747	792
42	a''	682	678
43	a''	577	532
44	a''	485	468
45	a''	430	390
46	a''	278	275
47	a''	189	186
48	a''	115	113

Table S1: Harmonic vibrational frequencies for the S_0 and L_a states of the 2-naphtholate anion (NPO^-) calculated at the CAM-B3LYP/aug-cc-pVDZ level of theory.

Mode	Symmetry	S_0	L_a	L_b
1	a'	3814	3808	3819
2	a'	3215	3234	3245
3	a'	3204	3223	3213
4	a'	3190	3213	3210
5	a'	3181	3197	3192
6	a'	3178	3189	3174
7	a'	3153	3154	3164
8	a'	1761	1737	1949
9	a'	1680	1616	1700
10	a'	1668	1589	1597
11	a'	1605	1573	1561
12	a'	1586	1511	1534
13	a'	1544	1490	1487
14	a'	1506	1433	1455
15	a'	1462	1403	1407
16	a'	1437	1374	1391
17	a'	1385	1361	1362
18	a'	1371	1352	1343
19	a'	1316	1290	1309
20	a'	1284	1267	1276
21	a'	1257	1233	1254
22	a'	1199	1193	1193
23	a'	1188	1182	1188
24	a'	1151	1116	1134
25	a'	1133	1108	1120
26	a'	1085	1082	1056
27	a'	962	953	942
28	a'	933	934	919
29	a'	855	837	848
30	a'	762	760	745
31	a'	702	701	684
32	a'	640	624	628
33	a'	544	538	541
34	a'	537	532	530
35	a'	510	506	497
36	a'	458	443	457
37	a'	337	331	329
38	a'	299	293	294
39	a'	154	153	154
40	a''	1011	934	1075
41	a''	1005	923	980
42	a''	965	911	923

43	a''	907	809	917
44	a''	865	803	835
45	a''	827	741	768
46	a''	801	719	740
47	a''	788	661	699
48	a''	697	650	660
49	a''	597	607	618
50	a''	552	541	503
51	a''	482	437	437
52	a''	436	306	384
53	a''	310	299	283
54	a''	199	177	164
55	a''	168	137	159
56	a''	80	69	82
57	a''	67	64	63

Table S2: Harmonic vibrational frequencies for the S_0 , L_a and L_b states of the 6-hydroxy-2-naphthoate anion (NPOO^-) calculated at the CAM-B3LYP/aug-cc-pVDZ level of theory.

3 Mechanism for formation of photoproduct from NPOO^-

To investigate the photoreaction of NPOO^- with SF_6 , we measured the relative yields of the photoreaction product (postulated to involve replacing the OH group by F) and SF_6^- as the SF_6 concentration was increased. Laser on/off difference ATDs recorded at $\lambda = 455$ nm show a growth in the relative yield of the photoreaction product compared to electron detachment (monitored through SF_6^- signal) with increasing SF_6 partial pressure (see Fig. S5). A plot of $[\text{photoproduct}]/[\text{SF}_6^-]$ versus the increase in the arrival time of the NPOO^- anions, which according to Blanc's law should be proportional to the SF_6^- partial pressure, is shown in Fig. S6. The shape of the curve is consistent with efficient capture of the detached electrons, even at low SF_6 pressures, but with the formation of the photoproduct requiring collisional encounters between excited NPOO^- molecules and SF_6 . Note that the tail in the SF_6^- peak extending towards shorter arrival time Fig. S5 (low SF_6 partial pressure), occurs because the mobile, photodetached electrons drift for substantial distances before being captured by SF_6 .

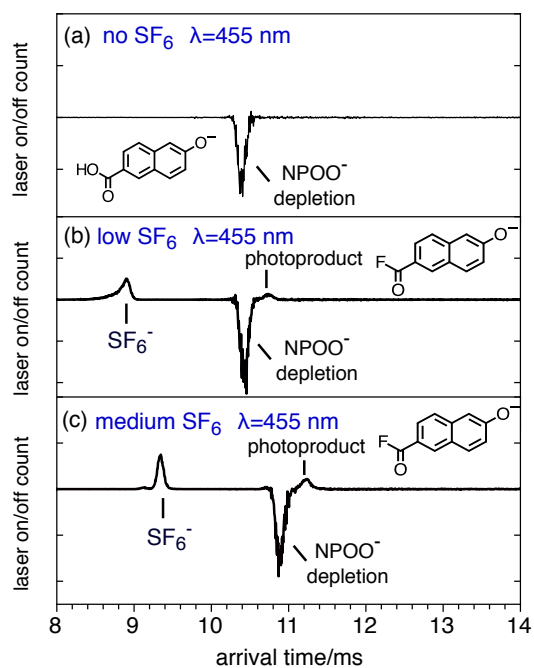


Figure S5: Laser on/off difference ATDs for NPOO^- showing formation of SF_6^- and the photoproduct that corresponds to replacement of OH group by F atom.

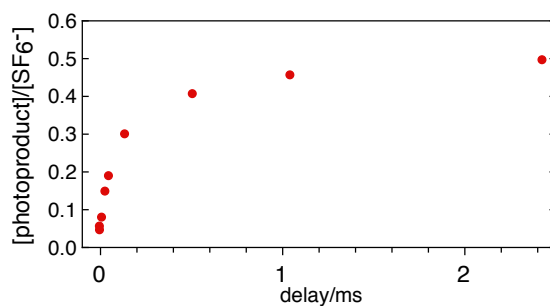


Figure S6: Relative yields of the photoproduct and SF_6^- as a function of the relative arrival time of the NPOO^- peak. Zero delay corresponds to no SF_6 in the drift tube.

4 Action spectra of naphtholate anions

Photodetachment action spectra of the naphtholate forms of deprotonated 2-naphthol, 1-naphthol, methylated 6-hydroxy-2-naphthoic acid, and 6-hydroxy-2-naphthoic acid obtained by monitoring the SF_6^- yield as a function of wavelength are shown in Fig. S7. All four action spectra span a similar wavelength range, although only the 2-naphtholate anion spectrum exhibits resolved vibronic structure.

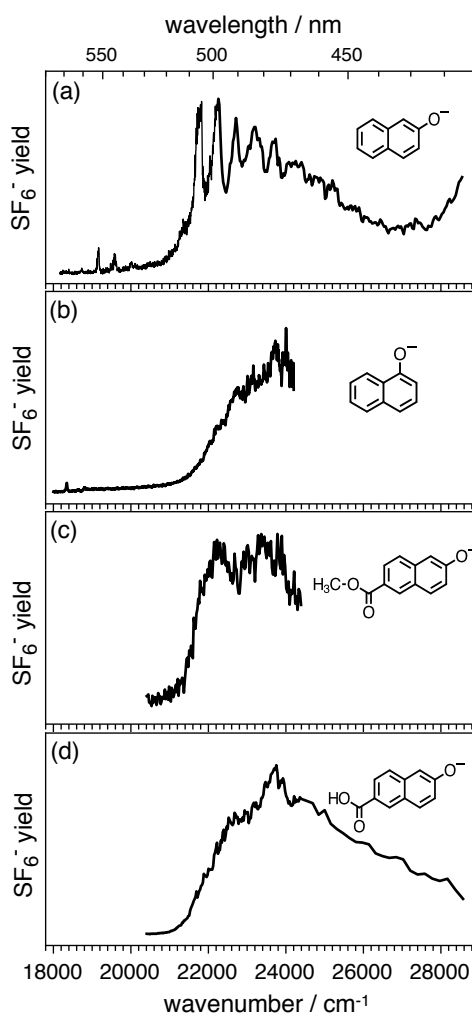


Figure S7: Photodetachment action spectra of the naphtholate forms of deprotonated 2-naphthol, 1-naphthol, methylated 6-hydroxy-2-naphthoic acid, and 6-hydroxy-2-naphthoic acid. The spectra were all generated by monitoring SF_6^- yield as a function of wavelength.

References

- [1] Y. Yang, E. R. Davidson and W. Yang, *Proc. Nat. Acad. Sci.*, 2016, **113**, E5098–E5107.
- [2] J. R. Platt, *J. Chem. Phys.*, 1949, **17**, 484–495.
- [3] T. Hashimoto, H. Nakano and K. Hirao, *J. Chem. Phys.*, 1996, **104**, 6244.
- [4] F. Bettanin, L. F. A. Ferrão, M. Pinheiro, A. J. A. Aquino, H. Lischka, F. B. C. Machado and D. Nachtigallova, *J. Chem. Theo. Comput.*, 2017, **13**, 4297–4306.
- [5] H. F. Bettinger, C. Tönshoff, M. Doerr and E. Sanchez-Garcia, *J. Chem. Theo. Comput.*, 2016, **12**, 305–312.
- [6] S. Grimme and M. Parac, *ChemPhysChem*, 2003, **4**, 292–295.
- [7] R. M. Richard and J. M. Herbert, *J. Chem. Theo. Comput.*, 2011, **7**, 1296–1306.
- [8] A. Prlj, M. E. Sandoval-Salinas, D. Casanova, D. Jacquemin and C. Corminboeuf, *J. Chem. Theo. Comput.*, 2016, **12**, 2652–2660.
- [9] O. Christiansen, H. Koch and P. Jørgensen, *J. Chem. Phys.*, 1995, **103**, 7429.
- [10] T. H. Dunning, Jr., *J. Chem. Phys.*, 1989, **90**, 1007.
- [11] M. Schreiber, M. R. Silva-Junior, S. P. A. Sauer and W. Thiel, *J. Chem. Phys.*, 2008, **128**, 134110.
- [12] D. Kállnár and P. G. Szalay, *J. Chem. Theo. Comput.*, 2014, **10**, 3757–3765.
- [13] T. Yanai, D. P. Tew and N. C. Handy, *Chem. Phys. Lett.*, 2004, **393**, 51–57.
- [14] F. Santoro, A. Lami, R. Improta, J. Bloino and V. Barone, *J. Chem. Phys.*, 2008, **128**, 224311.
- [15] G. J. Small, *J. Chem. Phys.*, 1971, **54**, 3300.
- [16] F. Negri and M. Z. Zgierski, *J. Chem. Phys.*, 1996, **104**, 3486.